J Soils Sediments
DOI 10.1007/s11368-017-1803-4

SEDIMENTS, SEC 2 • PHYSICAL AND BIOGEOCHEMICAL PROCESSES • RESEARCH ARTICLE

Sedimentary trace element sinks in a tropical upwelling system

Manuel Moreira[1] · Rut Díaz[1] · Helenice Santos[1] · Ursula Mendoza[1] · Michael E. Böttcher[2] · Ramses Capilla[3] · Ana L. Albuquerque[1] · Wilson Machado[1]

Received: 1 December 2016 / Accepted: 3 August 2017

Abstract
Purpose The accumulation of trace elements in sediments from highly productive continental margins may depend on the affinity of these elements for organic matter and their degrees of further incorporation into pyrite (FeS_2). We tested the hypothesis that the relative contributions of these geochemical phases play a substantial role as trace element (As, Cd, Cr, Cu, Mn, Ni, and Zn) sinks in the highly bioturbated sediments from the tropical upwelling system off Cabo Frio, southeastern Brazil.
Materials and methods Four sediment cores sampled across the Cabo Frio continental shelf were submitted to a sequential extraction procedure performed to separate three different operationally defined fractions, i.e., the geochemical phases soluble in 1 M HCl (considered as the "reactive" fraction), concentrated H_2SO_4 (considered as the organic matter-bound phase), and concentrated HNO_3 (considered as the pyrite-bound phase). The trace metal incorporation into pyrite was assessed by estimating the degree of trace metal pyritization (DTMP), while the pyrite sulfur stable isotope signatures ($\delta^{34}S_{Pyr}$) were used as proxies for sulfur redox cycling intensity.
Results and discussion Relative contributions of trace element fixation by organic matter and pyrite were positively correlated for Mn, Cr, and Ni on one hand, and negative correlated for Cu, on the other hand. The positive correlations imply in synergistic roles of these geochemical phases in determining the trace elements sedimentary sinks, while the negative relationship found for Cu reflects differences in the predominant retention mechanisms along with sediment burial. The $\delta 3^4S_{Pyr}$ signatures were negatively correlated with DTMP values of As, Cd, and Mn, suggesting a diminishing effect of the sulfur redox cycling on trace elements pyritization. These $\delta^{34}S_{Pyr}$ signatures were not correlated with DTMP values of Cr, Cu, and Ni, which were dominantly associated with the high organic matter contents found in this upwelling system.
Conclusions The role of pelagic organic matter scavenging of metals and later fueling of benthic microbial sulfate reduction and pyrite accumulation were evidenced as highly variable across the Cabo Frio shelf sediments. Differences in the organic matter accumulation in response to upwelling-enhanced primary productivity and in the intensity of bioturbation-driven sulfur redox cycling help to explain the spatial variability in the biogeochemical processes affecting the sedimentary trace metal sinks.

Keywords Degree of pyritization · Organic matter binding · Redox dynamics · Stable sulfur isotopes · Trace elements · Upwelling system

Responsible editor: Sophie Ayrault

Electronic supplementary material The online version of this article (doi:10.1007/s11368-017-1803-4) contains supplementary material, which is available to authorized users.

✉ Wilson Machado
wmachado@geoq.uff.br

[1] Projeto Ressurgência Team, Programa de Pós-Graduação em Geoquímica, Departamento de Geoquímica, Instituto de Química, Universidade Federal Fluminense, Niterói, RJ 24020-150, Brazil

[2] Geochemistry and Isotope Biogeochemistry Group, Marine Geology Department, Leibniz Institute for Baltic Sea Research (IOW), 18119 Warnemünde, Germany

[3] Petrobras/Cenpes/Geoquímica, Cidade Universitária, Ilha do Fundão, RJ 21941-915, Brazil

1 Introduction

The trace element (TE) accumulation in sediments from highly productive continental margins may be influenced by incorporation of these elements into organic matter derived from pelagic

Published online: 12 August 2017

primary producers (Acharya et al. 2015; Böning et al. 2015; Cheriyan et al. 2015). Some of these elements are biologically essential (e.g., Cu, Ni, Zn), which explains their affinity for organic matter and associated efficient scavenging to bottom sediments (Chaillou et al. 2002; Saito et al. 2002; Brumsack 2006; Muñoz et al. 2012). Concurrently to this well-known process of TE accumulation in continental margin sediments, the buried organic matter can fuel microbial sulfate reduction and the production of pyrite (FeS_2), which may constitute an additional TE sink, as recorded for a wide range of sedimentary environments (Raiswell and Plant 1980; Huerta-Diaz and Morse 1992; Dellwig et al. 2002; Neumann et al. 2013).

The mechanistic understanding of the processes controlling the incorporation of TE into pyrite is essentially based on an extension of the concept describing the conversion of reactive iron into pyrite (degree of pyritization, DOP; Berner 1970; Rickard and Luther 2007), the incorporation of TE into pyrite (degree of trace metal pyritization, DTMP; Huerta-Diaz and Morse 1990, 1992). The DTMP variability between elements is dependent on thermodynamic relationships (e.g., determining metal incorporation into pyrite or formation of metal monosulfides), but also reflect differences in ligand exchange reaction kinetics and redox reaction pathways (Morse and Luther 1999). The DTMP concept has successfully been applied in several modern sedimentary environments, ranging from shallow intertidal (e.g., Huerta-Diaz and Morse 1992) to deep continental slope sediments (e.g., Otero et al. 2003), and was extended to ancient euxinic environments (e.g., Berner et al. 2013). However, the TE geochemical partitioning in response to sedimentary boundary conditions is still not fully understood. There are comparatively few data on DTMP variability under the impact of sulfide oxidation (Morse et al. 1993; Cooper and Morse 1998; Machado et al. 2014; Noël et al. 2014), while there are experimental evidences of pyrite consumption under oxidizing conditions (Morse 1994a, b; Bataillard et al. 2014).

Coastal and marine sediments can present intense sulfur redox cycling, as indicated by stable sulfur isotope ($\delta^{34}S$) fractionation in sediment pore water sulfate and solid-phase sulfides in relation to seawater sulfate (Böttcher et al. 2000; Habicht and Canfield 2001; Wijsman et al. 2001). Figure 1 synthesizes the major processes involved in this cycling, which include a major role of dissimilatory sulfate reduction and disproportionation of sulfur intermediates in determining the $\delta^{34}S$ signals (Jørgensen 1990; Canfield et al. 1993; Canfield and Thamdrup 1994; Cypionka et al. 1998; Habicht et al. 1998; Pellerin et al. 2015). This sulfur cycling may include pyrite oxidation processes promoted by physical disturbances and bioturbation (Morse 1994a, b; Morse and Luther 1999; Otero et al. 2006; Aller et al. 2010; Diaz et al. 2012; Ding et al. 2014; Noël et al. 2014), whereas pyrite oxidation records can be also observed in ancient sedimentary environments (Soliman and El Goresy 2012). Besides the aerobic oxidative consumption of pyrite, anaerobic oxidation processes may be possibly also important, e.g., due to pyrite reactions with metal oxides (Schippers and Jørgensen 2001; Wu et al. 2016). Considering that pyrite-bound metals can be mobilized due to pyrite oxidation (Morse 1994a, b; Machado et al. 2011; Noël et al. 2015), the importance of pyrite as a TE sink may possibly change in response to this mobilization and new TE relative associations with different geochemical fractions (Fig. 1). However, the hypothesis that both organic matter and pyrite play major roles as TE carriers in bioturbated continental margin sediments from highly productive areas was not tested previously.

This study evaluates potential mechanisms involved in the TE accumulation in sediments from the upwelling system off Cabo Frio, southeastern Brazil, assessing the relative contributions of organic matter and pyrite as sinks for these elements. A previous work on this tropical system combined geochemical and sulfur isotopes data with micro-textural observation of pyrite surface to evaluate the impact of the sulfur redox cycling on the development of sulfur isotope signals in sediments sampled across the continental shelf (Diaz et al. 2012). This previous work evidenced an elevated isotopic fractionation between seawater sulfate and chromium-reducible sulfur (CRS, essentially pyrite), with the observed $\Delta^{34}S$ values (up to 60‰) revealing an intense sulfur cycling influenced by intense bioturbation. This sulfur redox cycling inference based on stable isotopes signatures is supported by the known significant discrimination of the stable sulfur isotopes due to successive dissimilatory sulfate reduction events, leading to an increasing enrichment of ^{32}S in the H_2S produced and in the derived pyrite (e.g., Chambers and Trudinger 1979; Wijsman et al. 2001; Diaz et al. 2012).

In the present study, previously reported Fe speciation and sulfur isotope results (Diaz et al. 2012) are combined with new data on DTMP values and new geochemical partitioning data for a number of TE (As, Cd, Cr, Cu, Mn, Ni, and Zn). This combination allowed us to test the hypotheses that (1) the organic matter and pyrite play synergistic roles as TE sinks and (2) the sulfur redox dynamics can limit the TE incorporation into pyrite along the Cabo Frio upwelling area.

2 Study area and methods

In April and May 2010, four box-cores were recovered from the continental shelf area off Cabo Frio (Fig. 2). Sub-cores were retrieved from these box-cores by using PVC tubes (Ø = 10 cm, 40-cm length). These sediment profiles were sliced in 1-cm-depth intervals and stored at 4 °C in acid-cleaned plastic containers until further laboratory processing. The oceanography of the study area is dominated by the warm (> 20 °C) tropical water (TW) flowing along the shelf border carried by the Brazil Current (BC), and the underlying relative cold (< 18 °C) South Atlantic Central Water (SACW). During intense NE winds driving upwelling events, the intrusion of SACW into the euphotic zone increases local primary productivity by enhancing nutrient input

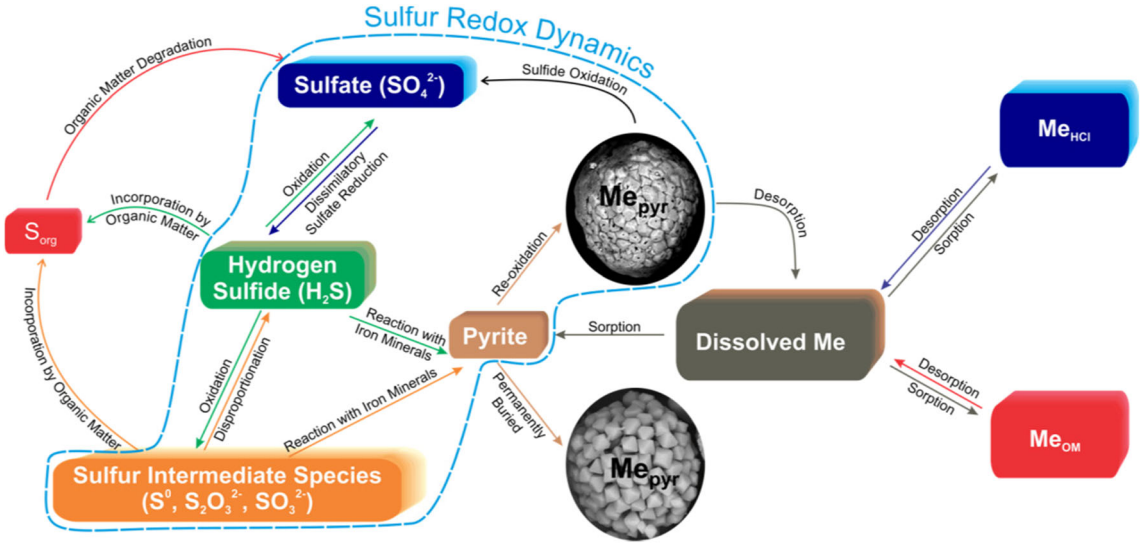

Fig. 1 Representation of the sulfur cycling, major processes involved and the trace metal cycling between the geochemical fractions that constitute the considered sedimentary metal sinks (i.e., organic matter-bound (Me_{OM}) and pyrite-bound (Me_{pyr}) metal fractions), and a "reactive" metal fraction, as conventionally obtained by diluted HCl extraction (Me_{HCl}). Me_{OM}, Me_{pyr}, and Me_{HCl} are defined according to Huerta-Diaz and Morse (1990)

to the euphotic zone (Albuquerque et al. 2014). In this highly productive system, the abundance of sedimentary pyrite in the studied surface sediments indicates that microbial sulfate reduction takes place. However, the observed bioturbation structures, essentially constant pore water sulfate concentrations and the absence of sulfide at all studied sites (Diaz et al. 2012) indicate the work of an efficient oxidative part of the sulfur cycle. Table 1 presents the main sedimentary characteristics of the sampling stations.

As described in detail by Huerta-Diaz and Morse (1990), a sequential trace element extraction procedure was performed, in order to separate different operationally defined fractions soluble in 1 M HCl (Me_{HCl}); concentrated H_2SO_4 (considered as organic matter-bound phases, Me_{OM}); and HNO_3 (considered as metals bound to pyrite, Me_{pyr}). Me_{OM} extraction was performed after removal of silicate phases with an extraction in 10 M HF. The determination of iron and TE concentrations was performed simultaneously, using a Jobin Yvon Ultima 2 sequential ICP-OES system. Analytical grade reagents obtained from Merck and Milli-Q water were used and analytical blank analyses were routinely performed. All used plastic and glassware were cleaned

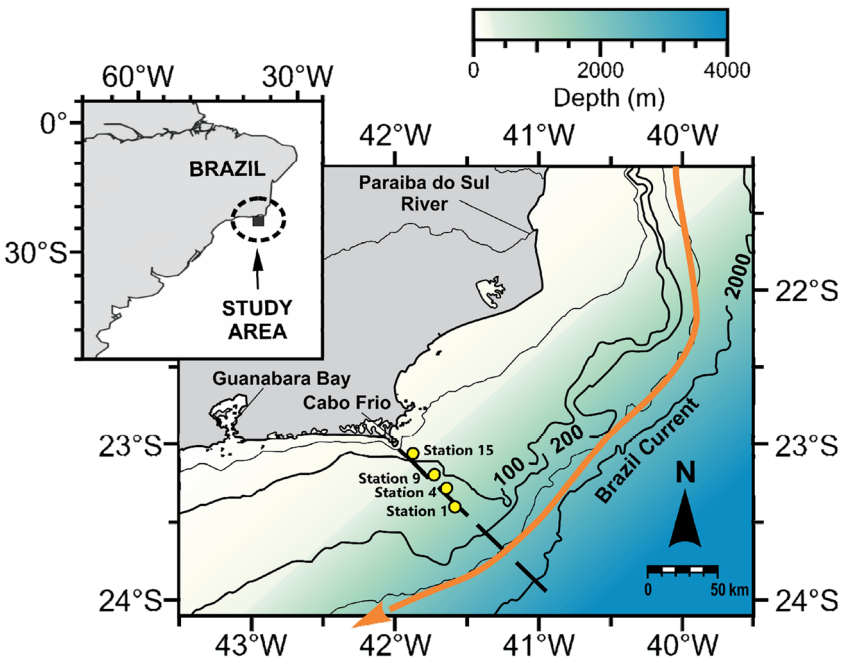

Fig. 2 Location of sampling stations in Cabo Frio upwelling area, southeastern Brazil

Table 1 Main characteristics of studied sediments

Sampling station	Core code	Location	Water depth (m)	Mud (%) (mean ± standard deviation)[a]	TOC (%) (median and range)[b]	TS (median and range)[b] (%)	CRS (%) (median and range)[b]	$\delta^{34}S_{CRS}$ (‰) (median and range)[b]	SR (mm year^{-1})[a]
Station 1	BCCF10-01	23° 40′ 38″ S, 41° 59′ 01″ W	128	58.7 ± 10.3	1.2 (1.0 to 2.0)	0.14 (0.004 to 0.29)	0.05 (0.006 to 0.24)	− 40 (− 42 to − 26)	1.0
Station 4	BCCF10-04	23° 27′ 64″ S, 41° 64′ 48″ W	120	89.5 ± 8.30	2.0 (1.5 to 2.3)	0.2 (0.05 to 0.31)	0.07 (0.007 to 0.16)	− 38 (− 41 to − 31)	1.4
Station 9	BCCF10-09	23° 20′ 13″ S, 41° 73′ 63″ W	117	92.3 ± 6.0	2.0 (1.6 to 2.6)	0.3 (0.03 to 0.32)	0.05 (0.01 to 0.14)	− 33 (− 39 to − 26)	1.8
Station 15	BCCF10-15	23° 05′ 86″ S, 41° 87′ 61″ W	79	61.1 ± 12.2	1.6 (1.1 to 2.2)	0.2 (0.14 to 0.31)	0.05 (0.02 to 0.08)	− 32 (− 36 to − 28)	5.5

TOC total organic carbon, *TS* total sulfur, *CRS* chromium reducible sulfur, $\delta^{34}S_{CRS}$ stable isotope ratio of CRS

[a] Data from Figueiredo et al. (2013). SR, sedimentation rate based on ^{210}Pb and $^{239+240}$Pu dating

[b] Data from Diaz et al. (2012)

with nitric acid (10%) for 24 h and further rinsed in Milli-Q water before use. DTMP values were calculated as defined by Huerta-Diaz and Morse (1990), according to Eq. 1:

$$DTMP = \left(Me_{pyr} \Big/ \left(Me_{HCl} + Me_{pyr}\right)\right) \times 100 \quad (1)$$

The DOP values were calculated using an equation analogous to that showed above for DTMP. There is no certified reference material for the chosen sequential extraction procedures that allow accuracy assessment. For an analytical reproducibility assessment, duplicate analysis of the certified reference material NRC PACS-2, Canada, was performed. The obtained analytical precision estimates were within ± 6% for all extraction procedures (Table S1, Electronic Supplementary Material). Note that the total concentrations of many elements (Fe, Mn, Cr, Cu) in the certified reference material were not well recovered by the sums of the three extraction procedures (Table S1, Electronic Supplementary Material). This may be expected since trace metal associations to heavy minerals that are not decomposed by the adopted sequential extraction scheme (determining Me_{HCl}, Me_{OM}, and Me_{Pyr}) may occur. Table S1 (Electronic Supplementary Material) also gives the analytical detection limits from different extraction procedures, while Table S2 (Electronic Supplementary Material) presents a synthesis of all results from each extraction step analyzed.

Data of chromium-reducible sulfur (CRS, essentially pyrite) and iron species (described above) were taken from Diaz et al. (2012), together with the sulfur isotope data of the CRS fraction ($\delta^{34}S_{CRS}$). The CRS extraction (CRS = FeS_2 + minor S^0) was performed using the two-step sequential distillation method from Fossing and Jørgensen (1989). The H_2S released from this extraction was collected in Zn-acetate trap, and the concentration of ZnS formed was measured by the colorimetric method described by Cline (1969). Contents of TOC (after carbonate removal by acidification) and total sulfur (TS) were determined by using a Eurovector elemental analyzer. For $\delta^{34}S_{CRS}$ analyses, the collected ZnS was converted to Ag_2S, washed, and dried. The isotope compositions of Ag_2S were measured by using combustion isotope ratio-monitoring gas mass spectrometry (Thermo Finnigan™ MAT 253). The $\delta^{34}S_{CRS}$ data are reported versus the international V-CDT standard in the conventional delta notation, which is equivalent to mU (Brand and Coplen 2012). A Pearson correlation analysis was performed, using a significance level of 0.05 as boundary criterion.

3 Results and discussion

Vertical profiles of contents and relative proportions of different geochemical fractions are presented in Figs. 3 and 4,

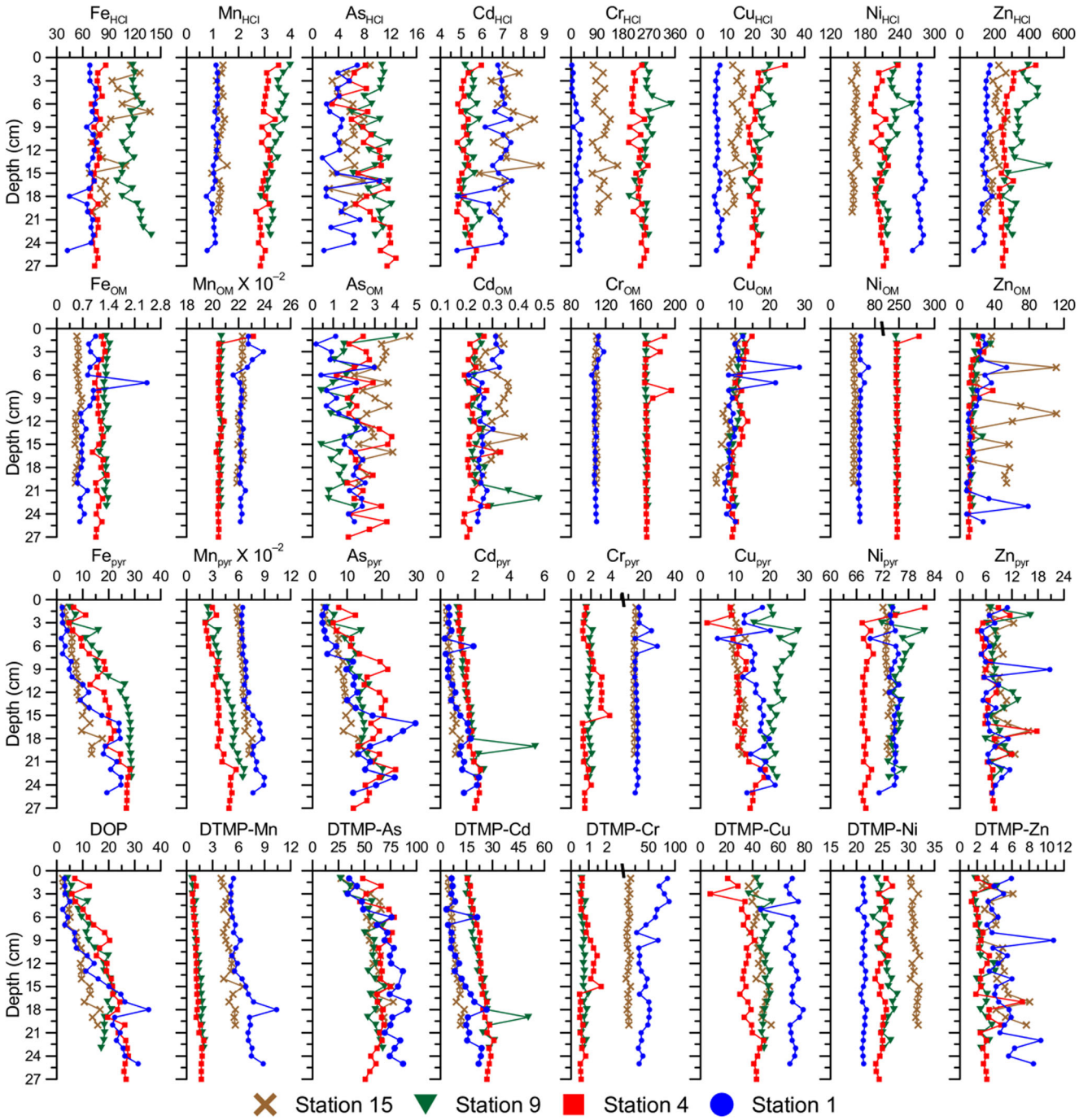

Fig. 3 Distribution of HCl-soluble and pyritic concentrations (μmol g^{-1} for Fe and Mn; nmol g^{-1} for other elements), degree of pyritization (DOP, %) and degree of trace metal pyritization (DTMP, %) in the studied sediment cores. Iron data (Fe_{HCl}, Fe_{pyr}, and DOP) are reproduced from Diaz et al. (2012), with permission

respectively, while metal concentration ranges per station are available in the Table S2 (Electronic Supplementary Material). Concentration profiles generally did not display clear vertical trends for HCl-soluble and organic matter-bound fractions, with the exception of the HCl-soluble Mn that decreased slightly with depth in stations 4 and 9, while many elements presented pyrite-bound concentration increases with depth (Fe, Mn, As, and Cd), which was not found for Cr, Cu, Ni, and Zn (Fig. 3). This observation suggests a clear trend of some trace elements to follow the Fe behavior of enrichment in the pyrite fraction, concurrently with a consumption of HCl-soluble Mn compounds within sediments from middle shelf (stations 4 and 9), along with diagenesis (e.g., Otero et al. 2003; Huerta-Diaz et al. 2011). This Mn consumption trend was associated with the smaller grain size and higher organic matter content found in stations 4 and 9 (Table 1), which can favor more intense diagenesis that can also

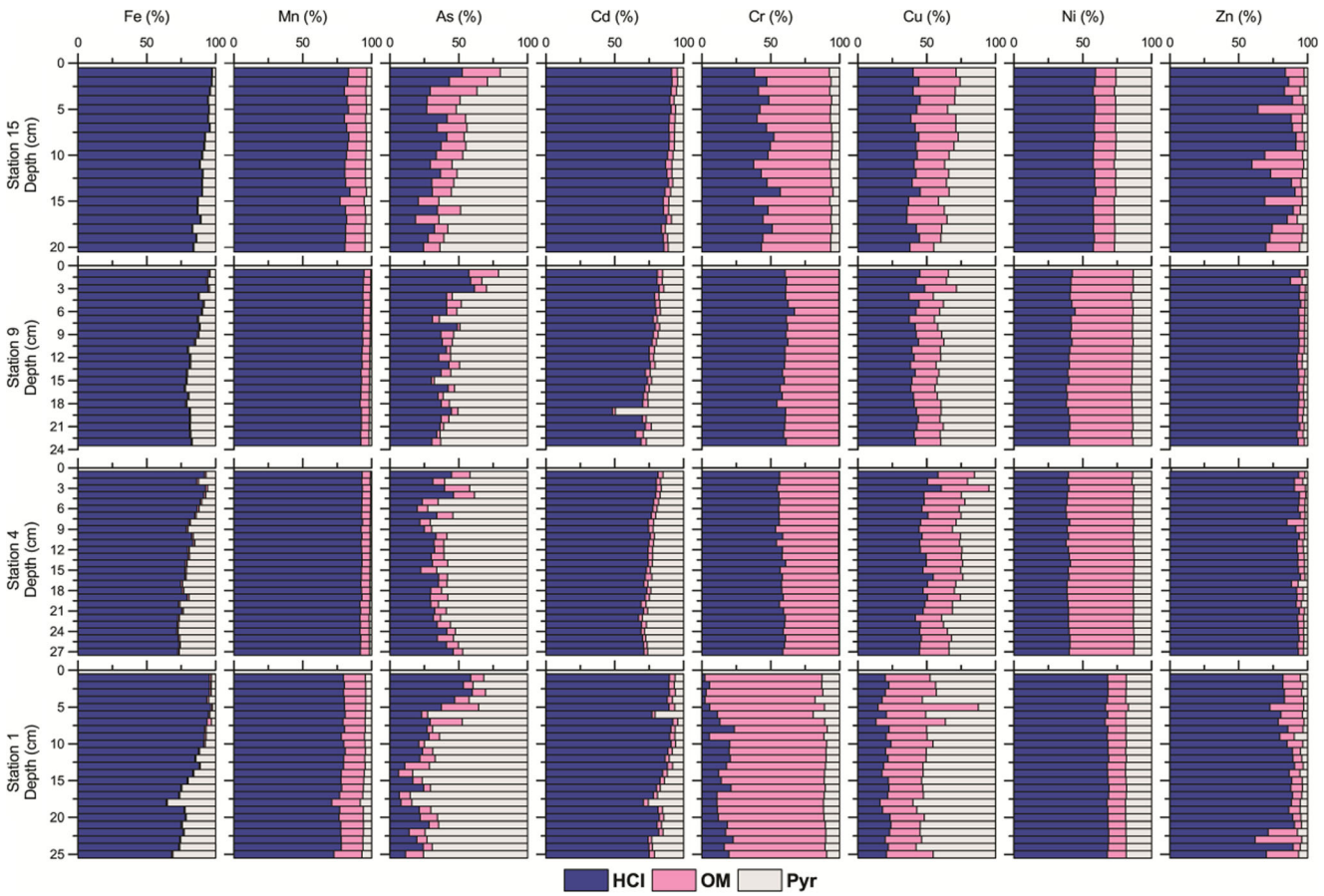

Fig. 4 Relative proportions (%) between the selected geochemical fractions of studied elements

explain the higher concentration of pyrite-bound Fe and Cd found in these stations (Fig. 3).

Iron pyritization increased with depth, which was followed by As and Cd DTMP values (Fig. 3). High DTMP values were observed for As (> 50%; Fig. 3), which is caused by the incorporation of As into pyrite (Huerta-Diaz and Morse 1992; Neumann et al. 2013). On the other hand, Mn, Cd, and Zn underwent only minor pyritization (< 30%), in agreement with previous observations (Morse and Luther 1999; Huerta-Diaz et al. 2011). The pyritization of Cu was highly variable (7–79%) close to the range reported in previous observation (Huerta-Diaz and Morse 1992; Huerta-Diaz et al. 2011). The top sediment layers at station 1 showed elevated DTMP values for Cr (up to 89%), contrasting with deeper layers (below 50%) and the other stations (< 18%) (Fig. 3). Exceptionally high DTMP (up to nearly 80%) has been reported for Cr elsewhere (Huerta-Diaz and Morse 1992; Morse et al. 1993), even though the chromate anion is kinetically inert to react with sulfide and is not predicted to be incorporated to substantial amounts into pyrite crystal lattice (Morse and Luther 1999).

Some TEs (Mn, Cd, and Zn) and Fe were predominantly found in the HCl-soluble fraction, while As was essentially bond to pyrite in all sampling positions across the shelf (Fig. 4). Though Cr, Cu, and Ni showed an abundance in highly variable geochemical fractions, they also show a relatively higher association with organic matter (~ 50–75% for Cr, ~ 25–40% for Cu, and ~ 20–50% for Ni) compared to the other elements (< 30%) (Fig. 4). These three essential metals are frequently associated to organic matter (e.g., Böning et al. 2004, 2015; Muñoz et al. 2012; Cheriyan et al. 2015; Noël et al. 2015). The Ni organic matter fraction was more important in the middle shelf positions (stations 4 and 9; Fig. 4), in association with the higher organic matter content found in these locations (Table 1). In opposition, lower organic matter fractions of Cr and Zn were observed in middle shelf stations, in which the HCl-fractions of these metals were predominant, following the Mn partitioning trend (Fig. 4). This can be explained by well-known associations of trace metals with Mn oxy-hydroxides (Shaw et al. 1990; Olson et al. 2017). Less variable contents in the organic matter fraction were observed for Cu, showing an enhanced variability of associations in the HCl-soluble and pyrite fractions (Fig. 4).

The behavioral contrasts between Cu and other elements may be partly due to some particularities of Cu chemistry, since this metal may occur either as Cu(I) and Cu(II) forms, resulting in a large variability of possible geochemical associations (e.g., multiple Cu sulfides may occur; Morse and Luther 1999). This allows the speculation that a variable affinity to be incorporated

by pyrite may be difficult generalizations on the Cu behavior under the dynamic physicochemical conditions found in the study area (as fueled by bioturbation-driven and hydrodynamics-driven process; Diaz et al. 2012), depending sedimentary heterogeneities (as exemplified by data from Table 1).

Concurrent TE associations to organic matter and pyrite were generally observed. This resulted in significant positive correlations (Fig. 5) between the proportions of organic matter bond and pyrite Mn (for all stations; $r = 0.59$ to 0.83), Cr (for stations 1 and 15; $r = 0.85$ and 0.96, respectively), and Ni (for stations 4 and 9; $r = 0.43$ and 0.55, respectively). In opposition, significant negative correlations occurred between the proportions of organic matter-bond and pyrite Cu in all stations ($r = -0.72$ to -0.97). The observed positive correlations can be explained by the fact that higher organic matter contents can stimulate the accumulation of pyrite and the pyritization of TE by sustaining a more intense microbial activity (e.g., Huerta-Diaz and Morse 1992; Müller 2002), while the accumulation of metals scavenged from the water column by particulate organic matter (e.g., Chaillou et al. 2002; Brumsack 2006) is concurrently favored. On the other hand, the negative relationship found for Cu was interpreted as derived from changes in the predominant mechanisms determining the Cu retention by sediments. The inverse variability in the importance of these two geochemical carriers was not necessarily dependent on depth for most stations, though station 15 presented a gradual increase in the relative importance of pyrite with depth, while the organic matter relative importance decreased (Fig. 4).

Many positive correlations between DTMP and DOP were observed (Fig. 6), which is statistically significant for Mn ($r = 0.75$ to 0.93); Cd ($r = 0.61$ to 0.96); As ($r = 0.68$ to 0.75, with the exception of data from station 4 that presented $r = 0.14$); and Cu ($r = 0.59$ to 0.80, with the exception of station 1 data that presented $r = 0.38$). Statistically significant correlations were generally not observed for Cr, Ni, and Zn, with a few exceptions in station 9 ($r = 0.66$ and 0.59 for Cr and Ni, respectively) and station 4 ($r = 0.47$ for Zn). Therefore, the expected trend of DTMP increases with increasing DOP, reflecting gradual incorporation into pyrite (Huerta-Diaz and Morse 1992), was frequently not observed. Previous efforts to elucidate the DTMP variability have often found absence of correlation with DOP for DTMP values, as reported for Mn, Cu, and Zn ($r < 0.15$) in anoxic fjord sediments (Müller 2002). However, changes in DOP and DTMP can result from alterations in the concentrations of TE in the pyrite and/or reactive phases, modifying DOP-DTMP relationships, e.g., in response to mechanisms of TE dissolution into sediment pore water and reincorporation by sediment solid phase (Ye et al. 2010, 2011). In this context, it is hypothesized that the described behavioral differences of TE in Cabo Frio shelf sediments may be influenced by the intense sulfur redox cycling previously identified in the same sampling sites, which possibly is a factor limiting the TE incorporation into pyrite in addition to those usually assessed in the literature.

The relationships of DOP and DTMP with $\delta^{34}S_{CRS}$ were evaluated to test the hypothesis that the intensity of sulfur cycling is associated with characteristic DTMP values (Fig. 7). The DTMP values for As (stations 1, 9, and 15); Mn (stations 1, 4, and 9); and Cd (all stations) are significantly correlated with the isotope composition of pyrite sulfur ($r = -0.95$ to -0.63). The same for Zn and Ni DTMP values was only observed at station 9 ($r = -0.72$ and -0.66, respectively) and for Cu at station 4 ($r = -0.74$). Moreover, the $\delta^{34}S_{CRS}$ threshold value for intense sulfur cycling assigned by Diaz et al. (2012) for the studied sediment cores is indicated in Fig. 7. This value was assigned considering that the CRS depletion in ^{34}S was largest and becomes less variable when CRS contents exceed ~ 0.1 wt%, with this threshold for intense sulfur cycling corresponding to a $\delta^{34}S_{CRS}$ average of $-40 \pm 1‰$ (Diaz et al. 2012). Below this threshold, increased DTMP values were observed for As, Cd, and Mn at station 1 (Fig. 7), as previously reported for DOP (Diaz et al. 2012). These results evidenced a diminishing effect on DTMP by the sulfur cycling, as revealed by $\delta^{34}S_{CRS}$ variability, which can affect the pyrite production and preservation against oxidation.

The proposed influence from the sulfur redox cycling on the TE incorporation and preservation into pyrite in Cabo Frio shelf sediments seems to be plausible to occur in a wide range of environments, considering that metal sulfide (including pyrite) oxidation is expected to occur due to ubiquitous processes, such as overlaying water oxygenation changes (Cooper and Morse 1996, 1998), bioturbation (Aller et al. 2010; Diaz et al. 2012),

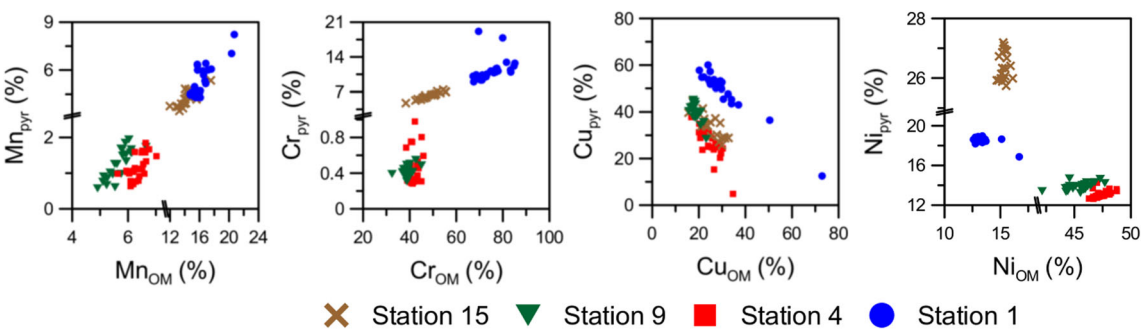

Fig. 5 Relationships between the proportions of organic matter-bond and pyrite-bound for Mn, Cr, Cu, and Ni

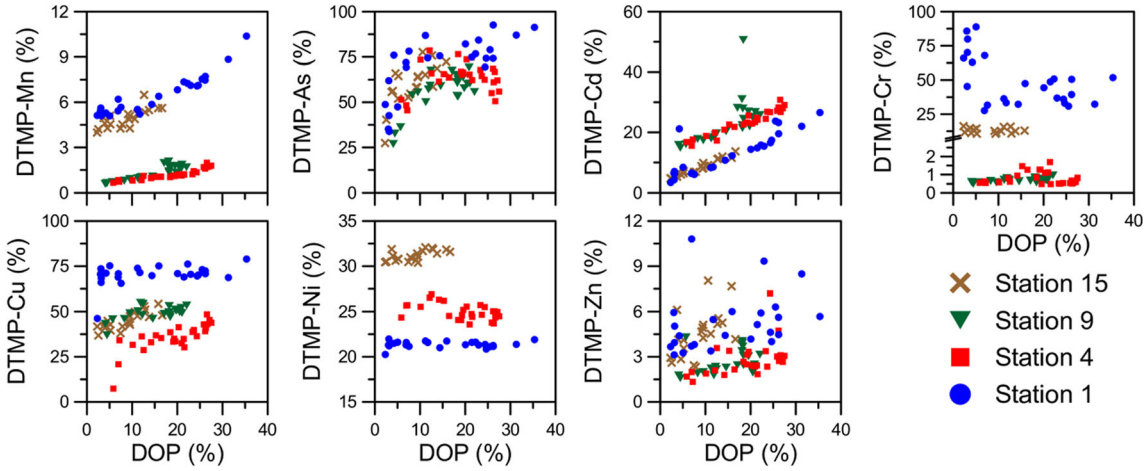

Fig. 6 Relationships between DTMP and DOP values

sediment re-suspension (Morse 1994a, b), and anaerobic oxidation (Aller and Rude 1988; Böttcher and Thamdrup 2001; Schippers and Jørgensen 2001), with possible contributions from sulfide-oxidizing bacteria (Böning et al. 2004; Sim et al. 2011). Elevated sulfur isotope fractionation between pore water sulfate and pyrite is frequently observed in systems under the impact of the oxidative part of the sulfur cycle, reaching strongly ^{34}S-depleted isotope signatures in modern environments (Habicht and Canfield 2001; Böning et al. 2004; Zopfi et al. 2008) and ancient sediments (Fisher 1986; Canfield and Teske 1996; Berner et al. 2013).

Relationships of sedimentary sulfur isotope signatures with metal contents have previously been described, e.g., with both total Mo and U contents (Dellwig et al. 2002) and with the Re/Mo ratios (Böning et al. 2004). Both positive and negative correlations of the Re/Mo ratio with pyrite δ^{34}S were found, depending on the position of the sediment in relation to the oxygen minimum zone off Peru (Böning et al. 2004). These observations indicate that the capacity of sediments to capture redox-sensitive TE may be enhanced by intense sulfur cycling and be reflected in sulfur isotope signature. A diminishing effect of sediment oxidation on DTMP was supposed by Morse et al. (1993) and Morse (1994a, b). In the case of sediment re-suspension events in a shallow coastal system, however, a positive effect on DOP and DTMP was proposed (Neumann et al. 2005; Scholz and Neumann 2007). In this later case, the authors concluded that intense oxidation may result in the formation of sulfur species with intermediate redox states, which may accentuate FeS conversion into pyrite according to the so-called polysulfide pathway (Rickard and Luther 2007). This suggests that the sulfur cycling may lead to both positive and negative effects on the degrees of DTMP.

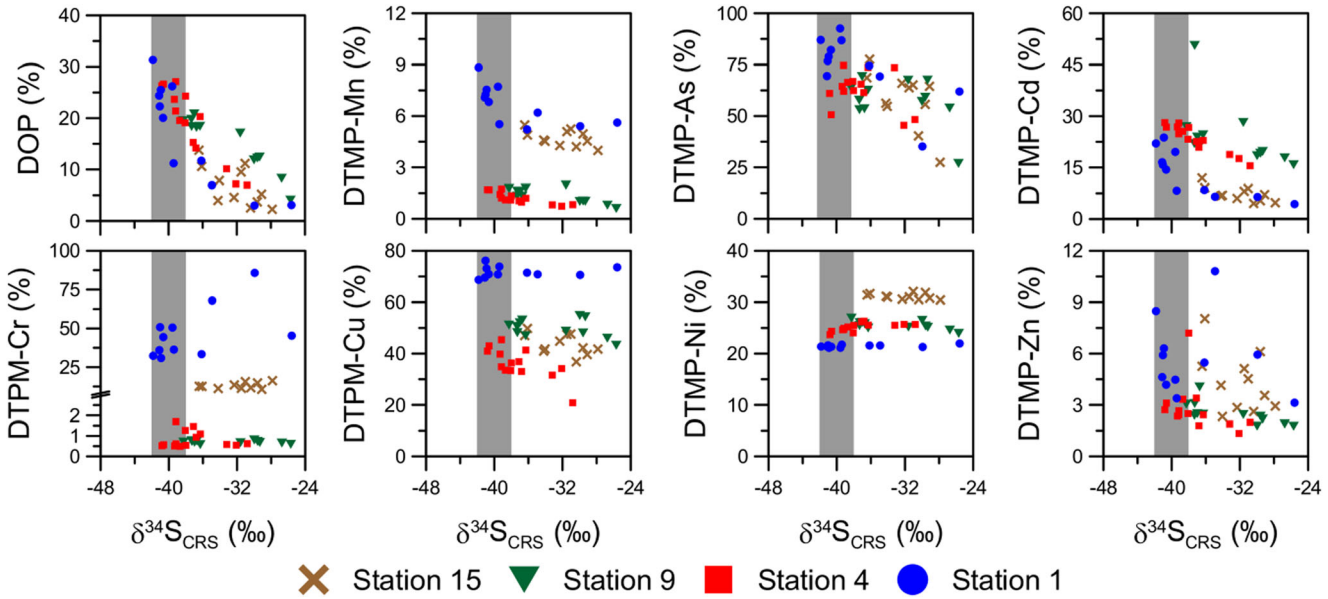

Fig. 7 Degree of trace metal pyritization (DTMP) plotted against $\delta^{34}S_{CRS}$. The shaded area corresponds to intervals below the threshold value for intense pyrite sulfur cycling, based on $\delta^{34}S_{CRS}$ signatures, as previously assigned by Diaz et al. (2012)

4 Conclusions

The relative importance of pyrite and organic matter as TE carrier were investigated in fine-grained and organic matter-rich sediments from the tropical Cabo Frio upwelling system, off Brazil. TE associations with pyrite were found in all cores, even under the conditions of intense bioturbation found in the study area. The relative contributions from organic matter and pyrite to determine the TE accumulation in these cores showed significant positive and negative correlations. While the positive relationships implied in the occurrence of a cumulative positive effect from pyrite and organic matter for Mn, Cr, and Ni, the negative correlation observed for Cu was associated to changes in the predominant mechanism of Cu retention. Significant covariations of DTMP with $\delta^{34}S_{CRS}$ indicate that the sulfur cycling may often lead to a diminished DTMP for As, Cd, and Mn, by limiting pyrite formation and preservation against oxidation. However, the elements that are associated with organic matter (Cr, Cu, and Ni) showed DTMP values decoupled from the change in $\delta^{34}S_{CRS}$. We conclude that DTMP values may result from more complex processes than usually considered, due to different sensitivities of specific elements to sulfur cycling. Besides the evident importance of pelagic organic matter scavenging of TE, the results give further evidence for the role of different organic matter sedimentations across the continental shelf that influence the development of DTMP values, fueling benthic sulfate reduction and pyrite formation.

Acknowledgements This work was funded by the Geochemistry Network of PETROBRAS/CENPES and the Brazilian National Petroleum and the Biofuels Agency (ANP). MM and RD received grants from Rio de Janeiro State Research Foundation (FAPERJ) and Brazilian Ministry of Education (CAPES). MEB received support from Leibniz IOW, and wishes to thank I. Scherff and P. Escher (IOW) for analytical support, and the late J.W. Morse for inspiring discussions.

References

Acharya SS, Panigrahi MK, Gupta AK, Tripathy S (2015) Response of trace metal medox proxies in continental shelf environment: the eastern Arabian sea scenario. Cont Shelf Res 106:70–84

Albuquerque ALS, Belém AL, Zuluaga FJB, Cordeiro LGM, Mendoza U, Knoppers BA, Gurgel MHC, Meyers PA, Capilla R (2014) Particle fluxes and bulk geochemical characterization of the Cabo Frio upwelling system in southeastern Brazil: sediment trap experiments between spring 2010 and summer 2012. An Acad Bras Cienc 86:601–620

Aller RC, Rude PD (1988) Complete oxidation of solid phase sulfides by manganese and bacteria in anoxic marine sediments. Geochim Cosmochim Acta 52:751–765

Aller RC, Madrid V, Chistoserdov A, Aller JY, Heilbrun C (2010) Unsteady diagenetic processes and sulfur biogeochemistry in tropical deltaic muds: implications for oceanic isotope cycles and the sedimentary record. Geochim Cosmochim Acta 74:4671–4692

Bataillard P, Grangeon S, Quinn P, Mosselmans F, Lahfid A, Wille G, Joulian C, Battaglia-Brunet F (2014) Iron and arsenic speciation in marine sediments undergoing a resuspension event: the impact of biotic activity. J Soils Sediments 14:615–629

Berner RA (1970) Sedimentary pyrite formation. Am J Sci 268:1–23

Berner ZA, Puchelt H, Noeltner T, Kramar U (2013) Pyrite geochemistry in the Toarcian Posidonia shale of south-west Germany: evidence for contrasting trace-element patterns of diagenetic and syngenetic pyrites. Sedimentology 60:548–573

Böning P, Brumsack H-J, Böttcher ME, Schnetger B, Kriete C, Kallmeyer J, Borchers SL (2004) Geochemistry of Peruvian near-surface sediments. Geochim Cosmochim Acta 68:4429–4451

Böning P, Shaw T, Pahnke K, Brumsack H-J (2015) Nickel as indicator of fresh organic matter in upwelling sediments. Geochim Cosmochim Acta 162:99–108

Böttcher ME, Thamdrup B (2001) Anaerobic sulfide oxidation and stable isotope fractionation associated with bacterial sulfur disproportionation in the presence of MnO_2. Geochim Cosmochim Acta 65: 1573–1581

Böttcher ME, Hespenheide B, Llobet-Brossa E, Beardsley C, Larsen O, Schramm A, Wieland A, Böttcher G, Berninger U-G, Amann R (2000) The biogeochemistry, stable isotope geochemistry, and microbial community structure of a temperate intertidal mudflat: an integrated study. Cont Shelf Res 20:1749–1769

Brand WA, Coplen TB (2012) Stable isotope deltas: tiny, yet robust signatures in nature. Isot Environ Health Stud 48:393–409

Brumsack H-J (2006) The trace metal content of recent organic carbon-rich sediments: implications for cretaceous black shale formation. Palaeogeogr Palaeoclimatol Palaeoecol 232:344–361

Canfield DE, Teske A (1996) Late Proterozoic rise in atomospheric oxygen concentration inferred from phylogenetic and sulphur-isotope studies. Nature 382:127–132

Canfield DE, Thamdrup B (1994) The production of ^{34}S-depleted sulfide during bacterial disproportionation of elemental sulfur. Science 266: 1973–1975

Canfield DE, Thamdrup B, Hansen JW (1993) The anaerobic degradation of organic matter in danish coastal sediments: iron reduction, manganese reduction, and sulfate reduction. Geochim Cosmochim Acta 57:3867–3883

Chaillou G, Anschutz P, Lavaux G, Schäfer J, Blanc G (2002) The distribution of Mo, U, and Cd in relation to major redox species in muddy sediments of the Bay of Biscay. Mar Chem 80:41–59

Chambers LA, Trudinger PA (1979) Microbiological fractionation of stable sulfur isotopes: a review and critique. Geomicrobiol J 1: 249–293

Cheriyan E, Sreekanth A, Mrudulrag SK, Sujatha CH (2015) Evaluation of metal enrichment and trophic status on the basis of biogeochemical analysis of shelf sediments of the southeastern Arabian Sea, India. Cont Shelf Res 108:1–11

Cline JD (1969) Spectrophotometric determination of hydrogen sulfide in natural waters. Limnol Oceanogr 14:70–82

Cooper D, Morse JW (1996) The chemistry of Offatts Bayou, Texas: a seasonally highly sulfidic basin. Estuar Coasts 19:595–611

Cooper DC, Morse JW (1998) Biogeochemical controls on trace metal cycling in anoxic marine sediments. Environ Sci Technol 32:327–330

Cypionka H, Smock AM, Böttcher ME (1998) A combined pathway of sulfur compound disproportionation in Desulfovibrio desulfuricans. FEMS Microbiol Lett 166:181–186

Dellwig O, Böttcher ME, Lipinski M, Brumsack H-J (2002) Trace metals in Holocene coastal peats and their relation to pyrite formation (NW Germany). Chem Geol 182:423–442

Diaz R, Moreira M, Mendoza U, Machado W, Böttcher ME, Santos H, Belém A, Capilla R, Escher P, Albuquerque AL (2012) Early diagenesis of sulfur in a tropical upwelling system, Cabo Frio, southeastern Brazil. Geology 40:879–882

Ding H, Yao S, Chen J (2014) Authigenic pyrite formation and re-oxidation as an indicator of an unsteady-state redox sedimentary environment: evidence from the intertidal mangrove sediments of Hainan Island, China. Cont Shelf Res 78:85–99

Figueiredo TS, Albuquerque ALS, Sanders CJ, Cordeiro LGMS, Silva-Filho EV (2013) Mercury deposition during the previous century in an upwelling region; Cabo Frio, Brazil. Mar Pollut Bull 76:389–393

Fisher ISJ (1986) Pyrite formation in bioturbated clays from the Jurassic of Britain. Geochim Cosmochim Acta 50:517–523

Fossing H, Jørgensen BB (1989) Measurement of bacterial sulfate reduction in sediments: evaluation of a single-step chromium reduction method. Biogeochemistry 8:205–222

Habicht KS, Canfield DE (2001) Isotope fractionation by sulfate-reducing natural populations and the isotopic composition of sulfide in marine sediments. Geology 29:555–558

Habicht KS, Canfield DE, Rethmeier J (1998) Sulfur isotope fractionation during bacterial reduction and disproportionation of thiosulfate and sulfite. Geochim Cosmochim Acta 62:2585–2595

Huerta-Diaz MA, Morse JW (1990) A quantitative method for determination of trace metal concentrations in sedimentary pyrite. Mar Chem 29:119–144

Huerta-Diaz MA, Morse JW (1992) Pyritization of trace metals in anoxic marine sediments. Geochim Cosmochim Acta 56:2681–2702

Huerta-Diaz MA, Delgadillo-Hinojosa F, Otero X, Segovia-Zavala J, Martin Hernandez-Ayon J, Galindo-Bect M, Amaro-Franco E (2011) Iron and trace metals in microbial mats and underlying sediments: results from Guerrero Negro Saltern, Baja California Sur, Mexico. Aquat Geochem 17:603–628

Jørgensen BB (1990) A thiosulfate shunt in the sulfur cycle of marine sediments. Science 249:152–154

Machado W, Rodrigues APC, Bidone ED, Sella SM, Santelli RE (2011) Evaluation of Cu potential bioavailability changes upon coastal sediment resuspension: an example on how to improve the assessment of sediment dredging environmental risks. Environ Sci Pollut Res 18:1033–1036

Machado W, Borrelli NL, Ferreira TO, Marques AGB, Osterrieth M, Guizan C (2014) Trace metal pyritization variability in response to mangrove soil aerobic and anaerobic oxidation processes. Mar Pollut Bull 79:365–370

Morse JW (1994a) Interactions of trace metals with authigenic sulfide minerals: implications for their bioavailability. Mar Chem 46:1–6

Morse JW (1994b) Release of toxic metals via oxidation of authigenic pyrite in resuspended sediments. In: Alpers CN, Blowes DW (eds) Environmental geochemistry of sulfide oxidation. American Chemical Society, Washington, DC, pp 289–297

Morse JW, Luther GW (1999) Chemical influences on trace metal-sulfide interactions in anoxic sediments. Geochim Cosmochim Acta 63: 3373–3378

Morse JW, Presley BJ, Taylor RJ, Benoit G, Santschi P (1993) Trace metal chemistry of Galveston Bay: water, sediments and biota. Mar Environ Res 36:1–37

Müller A (2002) Pyritization of iron and trace metals in anoxic fjord sediments (Nordåsvannet jord, western Norway). Appl Geochem 17:923–933

Muñoz P, Dezileau L, Lange C, Cardenas L, Sellanes J, Salamanca MA, Maldonado A (2012) Evaluation of sediment trace metal records as paleoproductivity and paleoxygenation proxies in the upwelling center off Concepción, Chile (36° S). Prog Oceanogr 92–95:66–80

Neumann T, Rausch N, Leipe T, Dellwig O, Berner Z, Böttcher ME (2005) Intense pyrite formation under low-sulfate conditions in the Achterwasser lagoon, SW Baltic Sea. Geochim Cosmochim Acta 69:3619–3630

Neumann T, Scholz F, Kramar U, Ostermaier M, Rausch N, Berner Z (2013) Arsenic in framboidal pyrite from recent sediments of a shallow water lagoon of the Baltic Sea. Sedimentology 60:1389–1414

Noël V, Marchand C, Juillot F, Ona-Nguema G, Viollier E, Marakovic G, Olivi L, Delbes L, Gelebart F, Morin G (2014) EXAFS analysis of iron cycling in mangrove sediments downstream a lateritized ultramafic watershed (Vavouto Bay, New Caledonia). Geochim Cosmochim Acta 136:211–228

Noël V, Morin G, Juillot F, Marchand C, Brest J, Bargar JR, Muñoz M, Marakovic G, Ardo S, Brown GE Jr (2015) Ni cycling in mangrove sediments from New Caledonia. Geochim Cosmochim Acta 169: 82–98

Olson L, Quinn KA, Siebecker MG, Luther GW, Hastings D, Morford JL (2017) Trace metal diagenesis in sulfidic sediments: insights from Chesapeake Bay. Chem Geol 452:47–59

Otero XL, Huerta-Diaz MA, Macías F (2003) Influence of a turbidite deposit on the extent of pyritization of iron, manganese and trace metals in sediments from the Guaymas Basin, gulf of California (Mexico). Appl Geochem 18:1149–1163

Otero XL, Calvo de Anta RM, Macías F (2006) Sulphur partitioning in sediments and biodeposits below mussel rafts in the Ría de Arousa (Galicia, NW Spain). Mar Environ Res 61:305–325

Pellerin A, Bui TH, Rough M, Mucci A, Canfield DE, Wing BA (2015) Mass-dependent sulfur isotope fractionation during reoxidative sulfur cycling: a case study from mangrove Lake, Bermuda. Geochim Cosmochim Acta 149:152–164

Raiswell R, Plant J (1980) The incorporation of trace elements into pyrite during diagenesis of black shales, Yorkshire, England. Econ Geol 75:684–699

Rickard D, Luther GW (2007) Chemistry of iron sulfides. Chem Rev 107: 514–562

Saito MA, Moppett J, Chisholm SW, Waterbury JB (2002) Cobalt limitation and uptake in Prochlorococcus. Limnol Oceanogr 47:1629–1636

Schippers A, Jørgensen BB (2001) Oxidation of pyrite and iron sulfide by manganese dioxide in marine ssediments. Geochim Cosmochim Acta 65:915–922

Scholz F, Neumann T (2007) Trace element diagenesis in pyrite-rich sediments of the Achterwasser lagoon, SW Baltic Sea. Mar Chem 107:516–532

Shaw TJ, Gieskes JM, Jahnke RA (1990) Early diagenesis in differing depositional environments: the response of transition metals in pore water. Geochim Cosmochim Acta 54:1233–1246

Sim MS, Bosak T, Ono S (2011) Large sulfur isotope fractionation does not require disproportionation. Science 333:74–77

Soliman MF, El Goresy A (2012) Framboidal and idiomorphic pyrite in the upper Maastrichtian sedimentary rocks at Gabal Oweina, Nile Valley, Egypt: formation processes, oxidation products and genetic implications to the origin of framboidal pyrite. Geochim Cosmochim Acta 90:195–220

Wijsman JWM, Middelburg JJ, Herman PMJ, Böttcher ME, Heip CHR (2001) Sulfur and iron speciation in surface sediments along the northwestern margin of the Black Sea. Mar Chem 74:261–278

Wu Z, Ren D, Zhou H, Gao H, Li J (2016) Sulfate reduction and formation of iron sulfide minerals in nearshore sediments from Qi'ao island, Pearl River estuary, southern China. Quatern Int. doi:10.1016/j.quaint.2016.06.003

Ye S, Laws EA, Wu Q, Zhong S, Ding X, Zhao G, Gong S (2010) Pyritization of trace metals in estuarine sediments and the controlling factors: a case in Jiaojiang estuary of Zhejiang Province, China. Environ Earth Sci 61:973–982

Ye S, Laws EA, Zhong S, Ding X, Pang S (2011) Sequestration of metals through association with pyrite in subtidal sediments of the Nanpaishui estuary on the western Bank of the Bohai Sea, China. Mar Pollut Bull 62:934–941

Zopfi J, Böttcher ME, Jørgensen BB (2008) Biogeochemistry of sulfur and iron in Thioploca-colonized surface sediments in the upwelling area off central Chile. Geochim Cosmochim Acta 72:827–843